Particle Collisions and Negative Nonlocal Response of Ballistic Electrons

Andrey Shytov, Jian Feng Kong, Gregory Falkovich, and Leonid Levitov

Phys. Rev. Lett. **121**, 176805 — Published 26 October 2018

DOI: 10.1103/PhysRevLett.121.176805

Particle Collisions and Negative Nonlocal Response of Ballistic Electrons

Andrey Shytov[a], Jian Feng Kong[b], Gregory Falkovich[c], Leonid Levitov[b]
[a] *School of Physics, University of Exeter, Stocker Road, Exeter EX4 4QL, United Kingdom*
[b] *Massachusetts Institute of Technology, Cambridge, Massachusetts 02139, USA and*
[c] *Weizmann Institute of Science, Rehovot, Israel*
(Dated: August 27, 2018)

An electric field that builds in the direction against current, known as negative nonlocal resistance, arises naturally in viscous flows and is thus often taken as a telltale of this regime. Here we predict negative resistance for the ballistic regime, wherein the ee collision mean free path is greater than the length scale at which the system is being probed. Therefore, negative resistance alone does not provide strong evidence for the occurrence of the hydrodynamic regime; it must thus be demoted from the rank of a smoking gun to that of a mere forerunner. Furthermore, we find that negative response is log-enhanced in the ballistic regime by the physics related to the seminal Dorfman-Cohen log divergence due to memory effects in the kinetics of dilute gases. The ballistic regime therefore offers a unique setting for exploring these interesting effects due to electron interactions.

Electron interactions can alter transport characteristics of solids in a variety of interesting ways[1]. In particular, electron systems in which momentum-conserving ee collisions dominate transport are expected to exhibit collective hydrodynamic flows[2–5]. Viscous electron fluids can harbor interesting collective behaviors akin to those of classical fluids[6–15]. Manifestations of electron hydrodynamics, predicted theoretically, provide guidance to experiments that attempt to demonstrate this regime[16–18]. One such manifestation, discussed recently[14, 16], is the "negative resistance" response i.e. current-induced electric field that builds in the direction against the applied current. In Ref.[14] negative resistance was predicted to arise naturally as the rate of momentum-conserving collisions exceeds the rate of momentum-relaxing collisions and the system transitions from the ohmic regime to the hydrodynamic regime. In Ref.[16] its observation was used as a signature of the hydrodynamic regime, taking it for granted that negative resistance is a fingerprint of the hydrodynamic regime. However, so far the smoking-gun status of this response has not been critically analyzed.

Here we show that negative resistance can occur not only in the hydrodynamic regime, when the ee collision mean free path l_{ee} is the smallest lengthscale in the system, but also in the ballistic regime, when l_{ee} is much greater than the lengthscales at which the system is being probed. This behavior is illustrated in Fig.1. As a result, negative resistance, taken alone, does not distinguish the hydrodynamic and ballistic regimes. Furthermore, the negative response value in the ballistic regime exceeds that in the hydrodynamic regime, which puts certain limitations on using this quantity as a diagnostic of hydrodynamics. However, the two regimes can be distinguished by the temperature and carrier density dependence of the response. As discussed below, the response strength grows with temperature in the ballistic regime and decreases in the viscous regime. Likewise, it shows different dependence on doping in the two regimes.

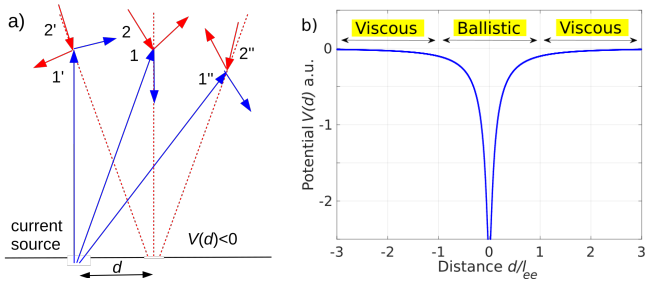

FIG. 1. Particles injected into an electron system from a current source (blue) undergo collisions with particles in the system bulk (red). The change in particle distribution is detected by a voltage probe at a distance r from the source, which measures particle flux into the boundary. The signal, dominated by ee interactions, is strongest at the distances smaller than the ee collision mean free path, $d \ll l_{ee}$. Panel (a) illustrates the mechanism of negative response: collisions between injected particles $1, 1', 1''$ and background particles $2, 2', 2''$ prevent some of the latter $(2', 2'')$ from entering the probe contact. Panel (b) shows the predicted dependence of the probe potential vs. distance.

These dependences, which are strikingly different in the two regimes, can provide guidance in delineating them in the existing[16, 19, 20] and future experiments.

The origin of negative resistance can be understood most easily by considering transport in the halfplane geometry wherein particles are injected from a point source placed at the boundary as shown in Fig.1a. In this case there are two competing contributions to be considered. First, the injected particles, after colliding with the background particles, can be reflected into voltage probe which measures particle flux into the boundary. This produces a positive contribution to the measured voltage response. Second, the same collision processes also prevent some of the background particles from entering the probe, producing a negative contribution to the measured signal. We will see that the latter effect dominates, resulting in the net signal of a negative sign.

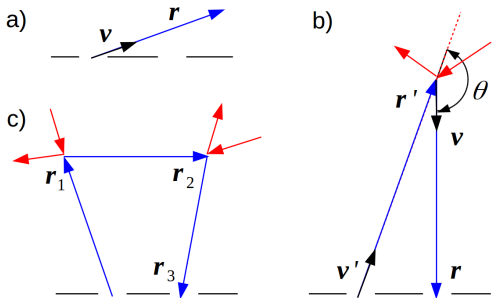

FIG. 2. Schematic illustration of different contributions to the nonlocal voltage response, arising in perturbation expansion of the solution of the transport equation, Eq.(4), in the ee collisions rate. Panels (a), (b) and (c), illustrate the 1st, 2nd and 3rd terms, respectively. The dominant contribution, which is of a negative sign, arises from the 2nd term (see text). In addition to the processes shown, an important contribution arises from the processes in which background particles are scattered away and prevented from entering the probe. Such "ghost" processes produce negative flux into the probe. These processes are pictured in Fig.1a (particles $1', 2'$ and $1'', 2''$).

Interestingly, when the ee mean free path l_{ee} is greater than the distance between the source and the probe d, all the lengthscales $d < r < l_{ee}$ contribute equally to the response. That is, the negative response is dominated by particles making a large excursion at $r > d$ before returning to the probe. In this case we find the behavior

$$V(d) \sim -J_0 \gamma_{ee} \ln \frac{l_{ee}}{d}, \qquad (1)$$

where J_0 is the injected current and γ_{ee} is the ee collision rate. As a function of distance, the response grows as d decreases, diverging as $d/l_{ee} \to 0$. This dependence is illustrated in Fig.1b. In contrast, it falls off and becomes very small at large d, remaining negative in both the hydrodynamic regime $d \gg l_{ee}$ and in the ballistic regime $d \ll l_{ee}$. Taken as a function of distance to the probe, the negative response is typically stronger in the ballistic regime than in the viscous regime.

The log enhancement arises due to a large phase space of contributing trajectories, which make long excursions to the distances up to l_{ee} and then are scattered back to the probe, as illustrated in Figs.1 and 2b. The long excursion times as well as the near-backscattering geometry of these trajectories give rise to strong magnetoresistance at anomalously weak magnetic fields. Estimates given below indicate that the threshold field values correspond to cyclotron radii on the order $R_c \sim l_{ee}^2/d \gg l_{ee}$, which can exceed typical sample dimensions.

The origin and behavior of the negative response bears strong resemblance to the seminal memory effects due to multiple correlated collisions in kinetic theory, discovered by Dorfman and Cohen, and others[21, 22]. This work made a surprising observation that virial expansion of the kinetic coefficients in gases breaks down due to multiple correlated collisions between two particles mediated by a third particle, which involve large excursions and log divergences similar to those found here. Manifestations of such memory effects, discussed so far, involved long-time power-law correlations in gases[23, 24]. Here, instead of three correlated collisions, similar effects arise from a single collision, with the current source and voltage probe playing the role of two other collisions. One can therefore view the log enhancement in Eq.1 as a direct manifestation of the memory effects predicted in kinetic theory.

Our transport problem can be readily analyzed with the help of the quantum kinetic equation

$$(\partial_t + \mathbf{v}\nabla - I_{ee})\, \delta f(\mathbf{r}, \mathbf{p}) = J_{\mathbf{r},\mathbf{p}}, \quad J_{\mathbf{r},\mathbf{p}} = J_0 \delta(\mathbf{r}). \qquad (2)$$

Here $\delta f(\mathbf{r}, \mathbf{p})$ describes particle distribution weakly perturbed near equilibrium. We assume $T \ll \epsilon_F$, in which case perturbed distribution is localized near the Fermi level and $\delta f(\mathbf{r}, \mathbf{p})$ can be parameterized as a function on the Fermi surface through the standard ansatz

$$\delta f(\mathbf{r}, \mathbf{p}) = -\frac{\partial f_0}{\partial \epsilon} \chi(\theta), \quad \chi(\theta) = \sum_m \chi_m e^{im\theta}, \qquad (3)$$

with f_0 the equilibrium Fermi-Dirac distribution and θ the angle parameterizing the Fermi surface. Due to cylindrical symmetry, the ee collision operator is in general diagonal in the angular harmonics basis (see below). The quantity $J_{\mathbf{r},\mathbf{p}}$ represents a current source placed at $\mathbf{r} = 0$. For conciseness, we ignore the angular anisotropy of the injected distribution.

The general solution of this equation is given by a formal perturbation expansion in the collision term

$$\delta f(\mathbf{r}, \mathbf{p}) = DJ_{\mathbf{r},\mathbf{p}} + DI_{ee}DJ_{\mathbf{r},\mathbf{p}} + DI_{ee}DI_{ee}DJ_{\mathbf{r},\mathbf{p}} + \ldots \qquad (4)$$

where $D = (\delta + \mathbf{v}\nabla)^{-1}$ is the Liouville propagator. Here, to describe a steady state, an infinitesimal positive δ was added in place of ∂_t to ensure that the steady-state response obeys causality. The collision processes described by this series are illustrated in Fig.2. The first term represents particles moving freely away from the source:

$$\delta f_1(\mathbf{r}, \mathbf{p}) = \int_0^\infty dt \delta^{(2)}(\mathbf{r} - \mathbf{v}t) J_0, \qquad (5)$$

where t is an auxiliary time parameter arising from solving transport equations as $\delta f_1 = \sum_{\mathbf{k}} e^{i\mathbf{k}\mathbf{r}} \frac{J}{\delta + i\mathbf{k}\mathbf{v}} = \sum_{\mathbf{k}} \int_0^\infty dt e^{i\mathbf{k}(\mathbf{r}-\mathbf{v}t)} J$. The particles described by Eq.(5) never make it to the probe (Fig.2a). Other terms in Eq.(4) can also be evaluated in a similar manner. The second term describes injected particles scattered once by the background particles (Fig.2b), giving

$$\delta f_2(\mathbf{r}, \mathbf{p}) = \sum_{\mathbf{r}', t, t'} \delta^{(2)}(\mathbf{r} - \mathbf{r}' - \mathbf{v}t) \sigma(\theta) \delta^{(2)}(\mathbf{r}' - \mathbf{v}'t') J_0, \qquad (6)$$

where $\sum_{\mathbf{r}', t, t'}$ denotes $\int_0^\infty \int_0^\infty dt dt' \int d^2 r'$, and the "scattering crosssection" σ describes the change of the distribution due to a scattering event. The crosssection dependence vs. the angle between the incoming and outgoing

velocities θ (see Fig.2b) can be inferred from the form of the collision operator $I_{\rm ee}$. For illustration, here we consider the simplest one-rate model of $I_{\rm ee}$ in which all nonconserved harmonics relax at equal rates,[4, 15]

$$I_{\rm ee}\delta f = -\gamma_{\rm ee}\left(\delta f - 2\hat{\mathbf{p}}\cdot\langle\hat{\mathbf{p}}'\delta f'\rangle_{\theta'} - \langle\delta f'\rangle_{\theta'}\right), \quad (7)$$

where the average $\langle ...\rangle_{\theta'}$ is over $\mathbf{p}'$ angles; δf and $\delta f'$ is a shorthand for $\delta f(\mathbf{p},\mathbf{r})$ and $\delta f(\mathbf{p}',\mathbf{r})$, respectively. The last two terms in Eq.(7), which ensure momentum and particle number conservation, give the angle dependence

$$\sigma(\theta) = \gamma_{\rm ee}(1+2\cos\theta). \quad (8)$$

The two terms in this expression have very different meanings: the first, isotropic, term describes addition of an incident particle after its velocity is randomized by collision, the second term describes momentum recoil of the background particles as a result of scattering.

Crucially, the crosssection θ dependence in Eq.(8) is such that σ is positive at small θ but is *negative* in an interval of size $2\pi/3$ which includes the scattering angle $\theta=\pi$. The contribution of this process to the flux into the probe is dominated by the values $\theta \approx \pi - O(d/r)$. This contribution originates from scattering processes at relatively large distances from the injector $r \gg d$, giving a negative value which is log-enhanced:

$$\delta V \sim J_0 \int_d^\infty \frac{d^2r'}{r'^2} e^{-r'/l_{\rm ee}} \sigma(\theta\approx\pi) \sim -J_0\gamma_{\rm ee}\ln\frac{l_{\rm ee}}{d}. \quad (9)$$

The log factor is large in the ballistic regime $l_{\rm ee} \gg d$.

The textbook estimate $\gamma_{\rm ee} \sim T^2/\epsilon_F^2$, where R^* is the effective Rydberg constant near ϵ_F and b is a numerical factor of order unity, indicates that the response grows with temperature and decreases with carrier density. This is in contrast to the negative response in the hydrodynamic regime, which is proportional to viscosity and thus scales inversely with $\gamma_{\rm ee}$[14]. The opposite signs of the dependence vs. temperature and carrier density may help distinguish the ballistic and hydrodynamic negative response types.

Higher-order terms in Eq.(4) describe multiple scattering. E.g. the third term gives a contribution to particle flux into the probe of the form (Fig.2c):

$$J_0\gamma_{\rm ee}^2 \int\int \frac{d^2r_1 d^2r_2 e^{-L//l_{\rm ee}}}{|\mathbf{r}_1||\mathbf{r}_2-\mathbf{r}_1||\mathbf{r}_3-\mathbf{r}_2|} \sim \gamma_{\rm ee}J_0, \quad (10)$$

where $L = |\mathbf{r}_1| + |\mathbf{r}_2-\mathbf{r}_1| + |\mathbf{r}_3-\mathbf{r}_2|$. This contribution is non-divergent in the limit $a \ll l_{\rm ee}$, and thus is subleading to the second term by a log factor.

By a similar dimensional argument one can show that nth order terms gives contributions

$$J_0\gamma_{\rm ee}^n \int ... \int \frac{d^2r_1 d^2r_2 ... d^2r_n}{|\mathbf{r}_1||\mathbf{r}_1-\mathbf{r}_2|...|\mathbf{r}_n-\mathbf{r}_{n-1}|} \sim \gamma_{\rm ee}^n \frac{l_{\rm ee}^{2n}}{l_{\rm ee}^{n+1}} \sim \gamma_{\rm ee}. \quad (11)$$

This behavior of higher-order terms, featuring identical scaling with $\gamma_{\rm ee}$, simply means that perturbation expansion is ill-defined and cannot be used to evaluate the response outside the ballistic regime. As noted above, the log divergence of the second term and the power-law divergence of higher-order terms are related to the seminal divergences found in the breakdown of the virial expansion in kinetic theory due to memory effects in multiple correlated collisions[21, 22].

We now proceed to show that the nonlocal resistance also remains negative outside the ballistic regime, that is at large distances $r \gg l_{\rm ee}$. To describe this regime we need to incorporate boundary scattering into the model. Momentum relaxation at the boundary is usually described by diffuse boundary conditions, leading to a cumbersome mathematical boundary value problem. Instead, to simplify the analysis, here we extend particle dynamics from the halfplane to the full plane, and model momentum relaxation on the line $y=0$ through adding an additional term to the collision operator as

$$I_{\rm ee} \to I_{\rm ee} + I_{\rm bd}, \quad I_{\rm bd}\delta f = -\alpha\delta(y)P'\delta f. \quad (12)$$

Here P' is a projection on the harmonics $m=\pm1$: $P'\delta f = 2\hat{\mathbf{p}}\cdot\langle\hat{\mathbf{p}}'\delta f(\mathbf{p}')\rangle_{\mathbf{p}'}$. The limit $\alpha\to\infty$ is expected to mimic the no-slip boundary conditions. Carrier distribution induced by an injector is described by

$$(\mathbf{v}\nabla - I_{\rm ee} + \alpha(\mathbf{r})P')\delta f(\mathbf{r},\mathbf{p}) = J_0\delta(\mathbf{r}). \quad (13)$$

The solution of this transport problem can be obtained in Fourier representation $\delta f(\mathbf{r},\mathbf{p}) = \sum_{\mathbf{k}} e^{i\mathbf{kr}}\delta f_{\mathbf{k}}(\mathbf{r})$:

$$(i\mathbf{kv} - I_{\rm ee} + \hat{\alpha}P')\delta f_{\mathbf{k}}(\mathbf{r}) = J_0, \quad \langle\mathbf{k}|\hat{\alpha}|\mathbf{k}'\rangle = \alpha\delta_{k_1-k_1'}, \quad (14)$$

where the delta function $\delta_{k_1-k_1'}$ reflects translational invariance of the line $y=0$ in the x direction.

Next, we transform to the angular harmonics basis (3). We formally solve Eq.(14) by a perturbation series in α:

$$|\delta f\rangle = \left(G - G\hat{\alpha}G + G\hat{\alpha}G\hat{\alpha}G - ...\right)|0\rangle J_0, \quad (15)$$

where, $G = 1/(i\mathbf{kv} - I_{\rm ee})$ is the free-space Greens function, $|0\rangle$ denotes the $m=0$ angular harmonic. For conciseness, we absorb P' into $\hat{\alpha}$ and suppress the $\partial f_0/\partial\epsilon$ factor. The first term represents a solution of Eq.(14) for a point source in free space and no momentum relaxation, $\alpha=0$. Other terms describe scattering at the line $y=0$. Because of P' projection, every encounter with the line generates a contribution of the form $e^{i\theta}+e^{-i\theta} = 2\cos\theta$. We can therefore replace Eq.(15) by an equivalent free-space problem with a line source

$$(ivk\cos(\theta-\theta_k) - I_{\rm ee})\,|\delta f\rangle = J_0(1 + w_{k_1}2\cos\theta). \quad (16)$$

Here θ is the velocity angle and θ_k is the vector $\mathbf{k}$ angle, $k_1 + ik_2 = ke^{i\theta_k}$. The term 1 represents the original point source at $\mathbf{r}=0$; the terms $w_{k_1}e^{\pm i\theta}$ represent a

source distributed on the $y = 0$ line (no k_2 dependence). The weights w_{k_1} are evaluated in the Supplement.

In the basis (3), the transport problem (16) is represented as a system of coupled equations

$$\frac{ikv}{2}\left(e^{i\theta_k}\chi_{m+1} + e^{-i\theta_k}\chi_{m-1}\right) + \gamma_m\chi_m = J_m, \qquad (17)$$

where γ_m are the eigenvalues of the operator $I_{\rm ee}$, which is diagonal in the basis (3), and J_m take values J_0 and $w_{k_1}J_0$ for $m = 0, \pm 1$ and zero otherwise. Here we used the identity $\cos(\theta - \theta_k) = \frac{1}{2}(e^{i(\theta-\theta_k)} + e^{-i(\theta-\theta_k)})$, interpreting the factors $e^{\pm i\theta}$ as shift operators $m \to m \mp 1$.

In our one-rate model the eigenvalues of $I_{\rm ee}$ are $\gamma_m = \gamma_{\rm ee}$ for $|m| > 1$, and zero otherwise. We will now show that in this case the coupled equations, Eq.(17), have a solution with the m dependence of an exponential form

$$\chi_m = e^{-im\theta_k} \times \begin{cases} c_1(-iz)^{m-1}, & m > 0 \\ c_0, & m = 0 \\ c_{-1}(-iz)^{-(m+1)}, & m < 0 \end{cases} \qquad (18)$$

with $|z| < 1$. Plugging it into Eq.(17) with any $m \neq 0, \pm 1$ gives an algebraic equation $\frac{vk}{2}\left(z - z^{-1}\right) + \gamma_{\rm ee} = 0$. This equation is solved by

$$z = e^{-\lambda}, \quad \sinh\lambda = \frac{\gamma_{\rm ee}}{kv}. \qquad (19)$$

The $m = \pm 1$ and $m = 0$ equations are

$$c_0 - izc_{\pm 1} = e^{\pm i\theta_k} w_{k_1} \frac{2J_0}{ikv}, \quad c_1 + c_{-1} = \frac{2J_0}{ikv}. \qquad (20)$$

These equations give values

$$c_0 = J_0 \frac{2w_{k_1}\cos\theta_k + iz}{ikv}, \quad c_{\pm 1} = J_0 \frac{z \mp 2w_{k_1}\sin\theta_k}{ikvz}. \qquad (21)$$

The full distribution can now be evaluated by carrying out the sum over m. This gives a closed-form expression

$$\delta f_{\mathbf{k}}(\theta) = c_0 + \frac{c_1 e^{i(\theta-\theta_k)}}{1 + ize^{i(\theta-\theta_k)}} + \frac{c_{-1}e^{-i(\theta-\theta_k)}}{1 + ize^{-i(\theta-\theta_k)}} \qquad (22)$$

where the three terms represent the contributions of the harmonics $m = 0$, $m > 0$ and $m < 0$, respectively.

We model the voltage probe as a small slit which measures the incoming particle flux (for geometry, see Fig.1):

$$V(d) = \frac{ew}{G}F, \quad F = \int_{-\pi}^{0} \frac{d\theta}{2\pi} v\sin\theta\chi(r,\theta), \qquad (23)$$

where the integration limits $-\pi < \theta < 0$ select particles which are incident on the boundary. Here w is the slit width, e is electron charge, $G = 4\frac{4e^2}{h}\frac{2w}{\lambda_F}$ is the slit conductance. Particles incident at an angle θ contribute to the flux with the weight $v\sin\theta$.

We evaluate voltage on the probe, Eq.(23), using the carrier distribution (22), Fourier transformed to real space. The flux for the distribution (22) can be analyzed by summing the contributions of different harmonics with the help of the identity

$$\int_{-\pi}^{0} \frac{d\theta}{2\pi} v\sin\theta e^{im\theta} = \begin{cases} \frac{v}{\pi(m^2-1)}, & m \text{ even} \\ \pm\frac{iv}{4}, & m \text{ odd}, m = \pm 1 \\ 0, & m \text{ odd}, m \neq \pm 1 \end{cases}. \qquad (24)$$

The resulting response, illustrated in Fig.1b, is negative in both the ballistic and the hydrodynamic regimes. It is more negative in the ballistic regime, $d \ll l_{\rm ee}$, than in the hydrodynamic regime, $d \gg l_{\rm ee}$. Therefore, the sign of the response does not distinguish between the two regimes. However, since in the ballistic regime the response scales as $\gamma_{\rm ee}$, whereas in the hydrodynamic regime it scales as $\gamma_{\rm ee}^{-1}$, the temperature and density dependence will be of opposite signs in the two cases, providing a clear distinction between the two regimes.

For monolayer graphene the negative response of ballistic electrons, derived above, is proportional to $\lambda_F\gamma_{\rm ee} \sim T^2/n$, decreasing with n and growing with T. Yet, for a viscous flow the response is proportional to η/n^2, where η is viscosity. The estimate $\eta = nmv_F l_{\rm ee}/4$ then predicts a density-independent response. Interestingly, the experimentally measured response decreases with n and grows with T at not-too-high temperatures[16], resembling the behavior expected for ballistic electrons.

Furthermore, the negative response is enhanced in the ballistic regime, owing to the large phase space of contributing trajectories that span the lengthscales $d < r < l_{\rm ee}$. As discussed above, there is an interesting analogy between this enhancement and the memory effects in multiple correlated collisions, which lead to the breakdown of the virial expansion in dilute gases[21–24]. Such memory effects can be directly probed in our system by applying a magnetic field. The required field values are very small: the threshold field, above which the response is suppressed, corresponds to large cyclotron radius values $R_c \sim l_{\rm ee}^2/d$ that can exceed a typical sample size.

For an estimate, taking $l_{\rm ee} = 1\,\mu$m and $d = 100\,$nm (and assuming a typical graphene carrier density of $n \sim 10^{12}\,{\rm cm}^{-2}$) gives $R_c \sim 10\,\mu$m. This corresponds to very small field values of about $B \lesssim 10\,$mT above which the negative response will be altered significantly. These values are much smaller than the characteristic field scale for the free-particle magnetotransport, for which R_c must be on the order of sample dimension. Strong magnetoresistance at weak magnetic fields arises because the trajectories contributing to the negative response originate from near-backscattering processes (see Fig.1 and 2b). Such trajectories are easily deflected away from the probe even by a weak B field such that its cyclotron radius $R_c \sim l_{\rm ee}^2/d$ is much greater than the $l_{\rm ee}$ and d lengthscales. The ballistic regime in combination with magnetotransport therefore provides an ideal setting in which these effects due to electron interactions can be realized and explored.

[1] E. M. Lifshitz and L. P. Pitaevskii, *Physical Kinetics* (Pergamon Press, New York,1981)

[2] K. Damle and S. Sachdev, Nonzero-temperature transport near quantum critical points. *Phys. Rev. B* 56: 8714-8733 (1997).

[3] R. N. Gurzhi, Hydrodynamic Effects in Solids at Low Temperature. *Usp. Fiz. Nauk* **94**, 689-718 (1968).

[4] M. J. M. de Jong and L. W. Molenkamp, Hydrodynamic electron flow in high-mobility wires. *Phys. Rev. B* 51:13389-13402 (1985).

[5] R. Jaggi, Electron-fluid model for the dc size effect. *J. Appl. Phys.* 69:816-820 (1991).

[6] M. Müller, J. Schmalian and L. Fritz, Graphene: A Nearly Perfect Fluid. *Phys. Rev. Lett.* 103:025301 (2009).

[7] A. V. Andreev, S. A. Kivelson and B. Spivak, Hydrodynamic Description of Transport in Strongly Correlated Electron Systems. *Phys. Rev. Lett.* 106:256804 (2011).

[8] D. Forcella, J. Zaanen, D. Valentinis and D. van der Marel, Electromagnetic properties of viscous charged fluids. *Phys. Rev. B* 90:035143 (2014).

[9] A. Tomadin, G. Vignale and M. Polini, Corbino Disk Viscometer for 2D Quantum Electron Liquids. *Phys. Rev. Lett.* 113:235901 (2014).

[10] D. E. Sheehy and J. Schmalian, Quantum Critical Scaling in Graphene. *Phys. Rev. Lett.* 99:226803 (2007).

[11] L. Fritz, J. Schmalian, M. Müller and S. Sachdev, Quantum critical transport in clean graphene. *Phys. Rev. B* 78:085416 (2008) .

[12] B. N. Narozhny, I. V. Gornyi, M. Titov, M. Schütt and A. D. Mirlin, Hydrodynamics in graphene: Linear-response transport. *Phys. Rev. B* 91:035414 (2015).

[13] A. Cortijo, Y. Ferreirós, K. Landsteiner and M. A. H. Vozmediano, Hall viscosity from elastic gauge fields in Dirac crystals. *Phys. Rev. Lett.* 115:177202 (2015).

[14] L. Levitov and G. Falkovich, Electron viscosity, current vortices and negative nonlocal resistance in graphene Nature Phys. **12**, 672-676 (2016).

[15] H. Guo, E. Ilseven, G. Falkovich and L. Levitov, Higher-than-ballistic conduction of viscous electron flows. *Proc. Natl. Ac. Sci.* 114:3068-3073 (2017).

[16] D. A. Bandurin *et al.* Negative local resistance caused by viscous electron backflow in graphene. *Science* 351:1055-1058 (2016).

[17] J. Crossno *el.* Observation of the Dirac fluid and the breakdown of the Wiedemann-Franz law in graphene. *Science* 351:1058-1061 (2016).

[18] P. J. W. Moll, P. Kushwaha, N. Nandi, B. Schmidt and A. P. Mackenzie, Evidence for hydrodynamic electron flow in $PdCoO_2$. *Science* 351:1061-1064 (2016).

[19] A. I. Berdyugin *et al.* Measuring Hall Viscosity of Graphene's Electron Fluid arXiv:1806.01606

[20] D. A. Bandurin *et al.* Probing Maximal Viscous Response of Electronic System at the Onset of Fluidity arXiv:1806.0323

[21] J. R. Dorfman and E. G. D. Cohen, On the density expansion of the pair distribution function for a dense gas not in equilibrium. Phys. Lett. 66, 124 (1965).

[22] R. Peierls, Surprises in Theoretical Physics (Princeton Series in Physics, 1979)

[23] J. R. Dorfman and E. G. D. Cohen, Velocity Correlation Functions in Two and Three Dimensions Phys. Rev. Lett. 25, 1257 (1970).

[24] A. Dmitriev, M. Dyakonov and R. Jullien, Non-Boltzmann classical correction to the velocity autocorrelation function for isotropic scattering in two dimensions. Phys. Rev. B 71, 155333 (2005)